Electronic Supplementary Material (ESI) for Journal of Materials Chemistry A.
This journal is © The Royal Society of Chemistry 2016

Supplementary Information

Guanidinium nonaflate as a solid-state proton conductor

Xiaoli Chen,[a] Haolin Tang,*[a], Tristan Putzeys,[b] Jeroen Sniekers,[c] Michael Wübbenhorst,[b] Koen Binnemans,[c] Jan Fransaer,[d] Dirk E. De Vos,[e] Qingfeng Li[f] and Jiangshui Luo*[def]

[a]*State Key Laboratory of Advanced Technology for Materials Synthesis and Processing, Wuhan University of Technology, Wuhan 430070, P. R. China. E-mail: thln@whut.edu.cn*

[b]*Department of Physics and Astronomy, KU Leuven, Leuven 3001, Belgium.*

[c]*Department of Chemistry, KU Leuven, Leuven 3001, Belgium.*

[d]*Department of Materials Engineering, KU Leuven, Leuven 3001, Belgium. E-mail: jiangshui.luo@kuleuven.be*

[e]*Centre for Surface Chemistry and Catalysis, KU Leuven, Leuven 3001, Belgium.*

[f]*Department of Energy Conversion and Storage, Technical University of Denmark, Kgs. Lyngby 2800, Denmark.*

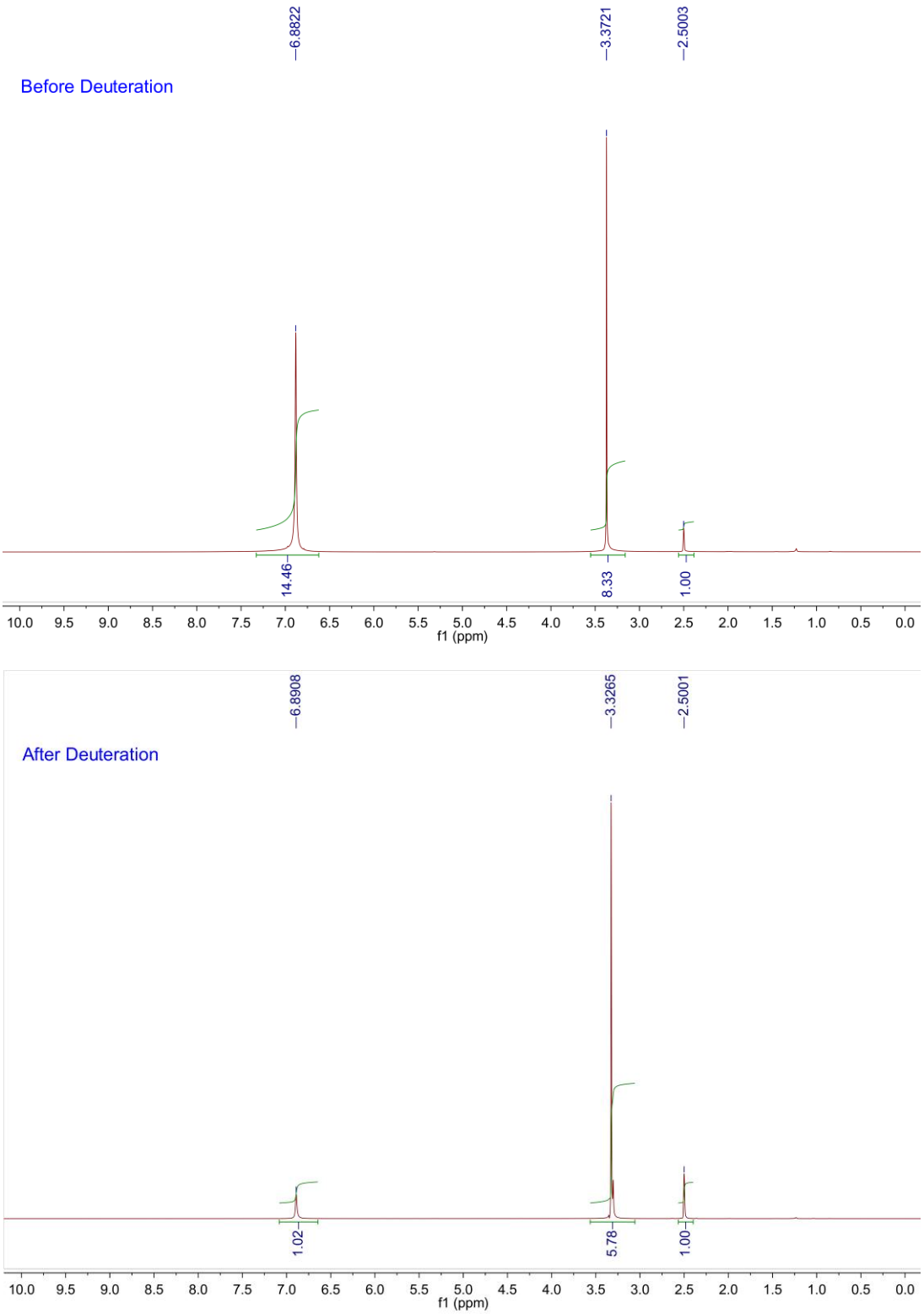

Fig. S1 ^{1}H NMR spectra of [Gdm-H][NfO] and [Gdm-D][NfO] (full ppm range). The signals of acidic hydrogens arise at 6.88 ppm (C−NH_2) in [Gdm-H][NfO] and 6.89 ppm (C−NHD) in [Gdm-D][NfO]. From the relative integration areas of the peaks for acidic hydrogens versus the peak area at 2.5 ppm (solvent), the deuteration percentage of acidic hydrogens in [Gdm-D][NfO] was estimated to be about (14.46−1.02)/14.46 × 100% = 92.9%. Note that the solvent was DMSO-d_6 and the concentration of the samples was controlled to be the same.

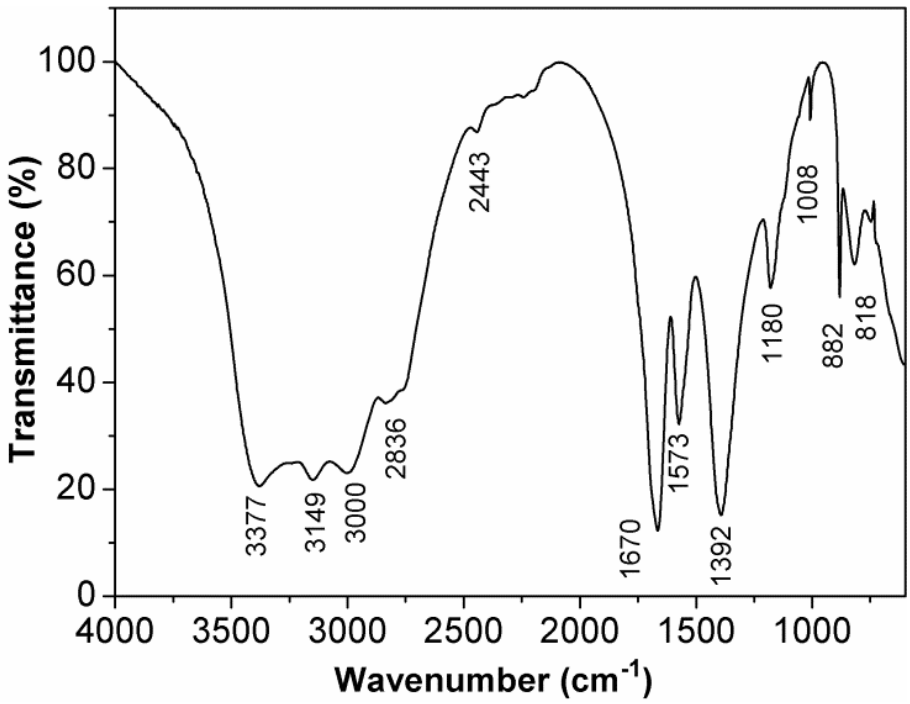

Fig. S2 FTIR spectrum of guanidine carbonate (KBr pellet), which agrees well with the reported spectrum of guanidine carbonate in the form of KBr disc.[1]

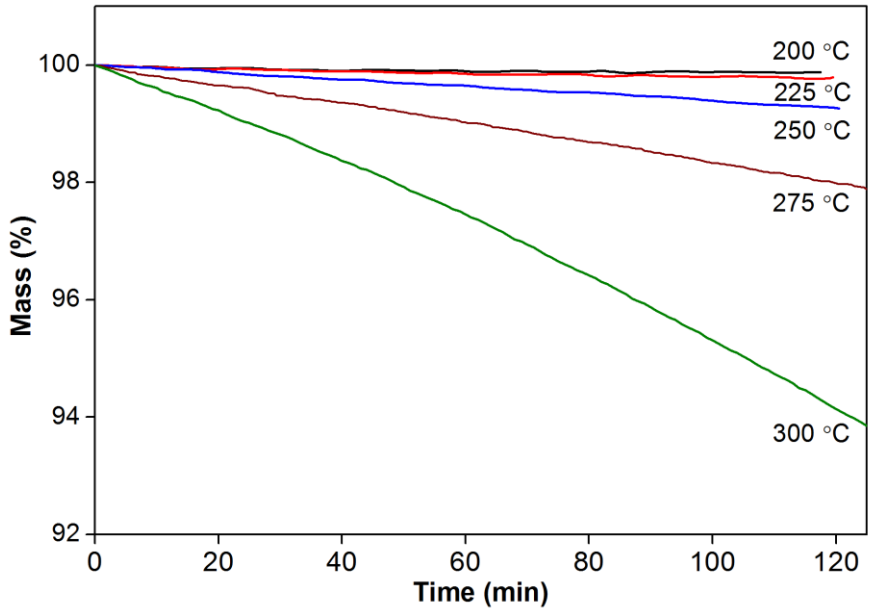

Fig. S3 Isothermogravimetric analysis of [Gdm-H][NfO] at five discrete temperatures under nitrogen purge (60 mL min^{-1}). Mass loss rate (expressed as the change in mass percent with time, $d\alpha/dt = (dm/dt)/m_0$, where m_0 is the initial mass): $d\alpha/dt$ = 0.0008437% min^{-1} at T = 200 ℃ with m_0 = 6.04 mg; $d\alpha/dt$ = 0.0017% min^{-1} at T = 225 ℃ with m_0 = 6.67 mg; $d\alpha/dt$ = 0.00606% min^{-1} at T = 250 ℃ with m_0 = 6.10 mg; $d\alpha/dt$ = 0.01718% min^{-1} at T = 275 ℃ with m_0 = 15.46 mg; $d\alpha/dt$ = 0.05263% min^{-1} at T = 300 ℃ with m_0 = 15.50 mg. Note that $dm/dt = m_0(d\alpha/dt)$.

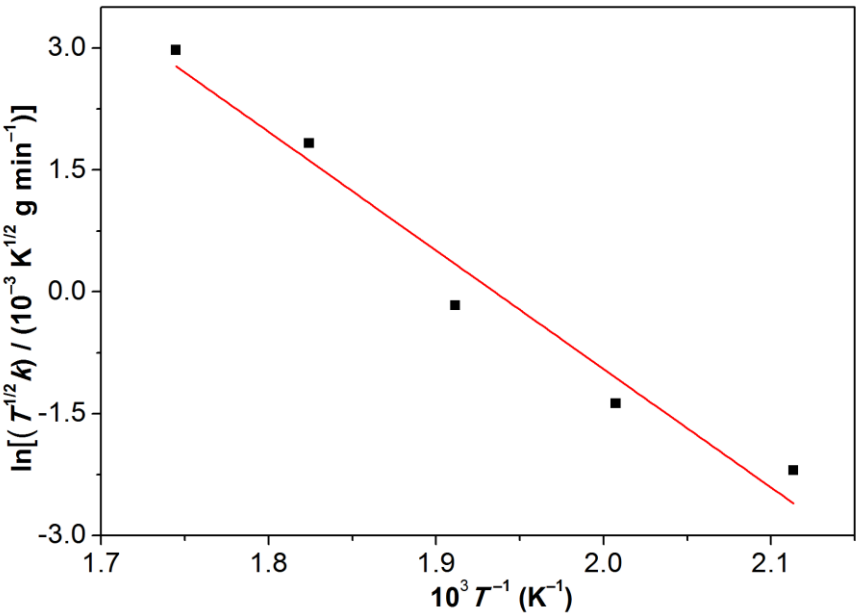

Fig. S4 Temperature dependence of the mass loss for [Gdm-H][NfO] based on the IGA results shown in Fig. S3. Such as plot yields a slope of $-\Delta_{vap}H/(1000R)$, where $\Delta_{vap}H$ is the enthalpy of vaporization, R is the universal gas constant, and k equals to $dm/dt = m_0(d\alpha/dt)$, which is the rate of mass loss per unit area shown in eqn. 3. Correlation of coefficient (R^2): 0.95653. $\Delta_{vap}H$ = 121.3 kJ mol^{-1}.

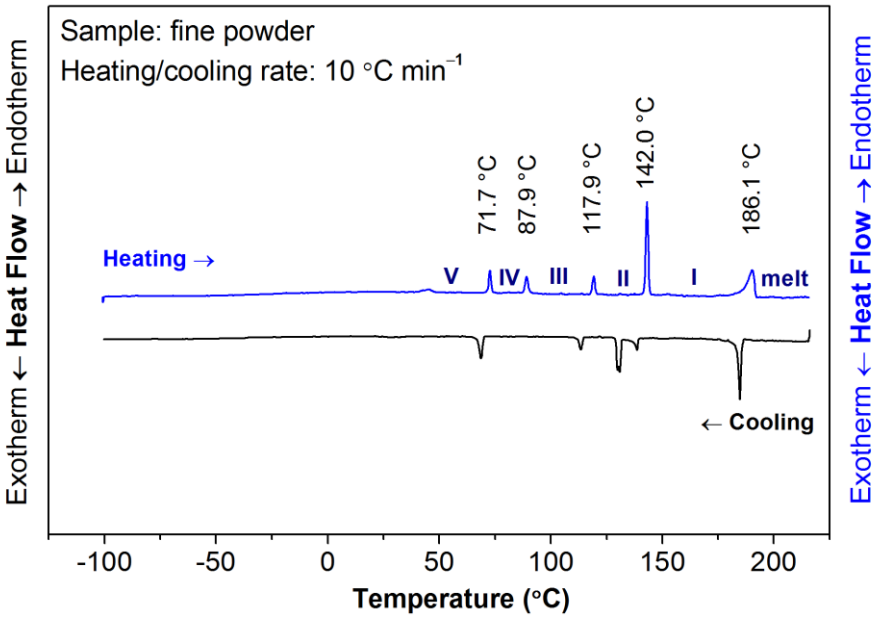

Fig. S5 DSC thermograms of [Gdm][NfO] measured at a scan rate of 10 ℃ min^{-1} for both heating and cooling scans.

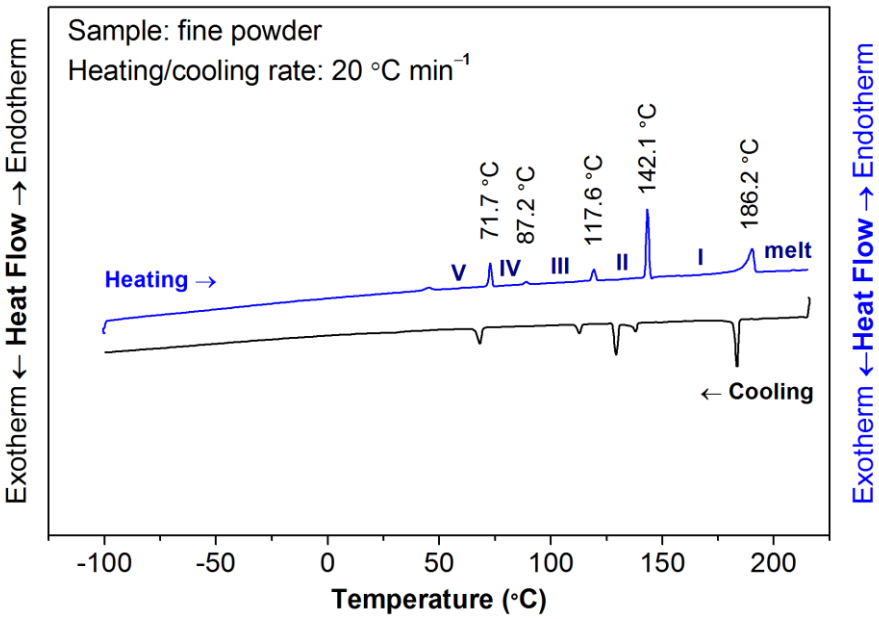

Fig. S6 DSC thermograms of [Gdm][NfO] measured at a scan rate of 20 ℃ min^{-1} for both heating and cooling scans.

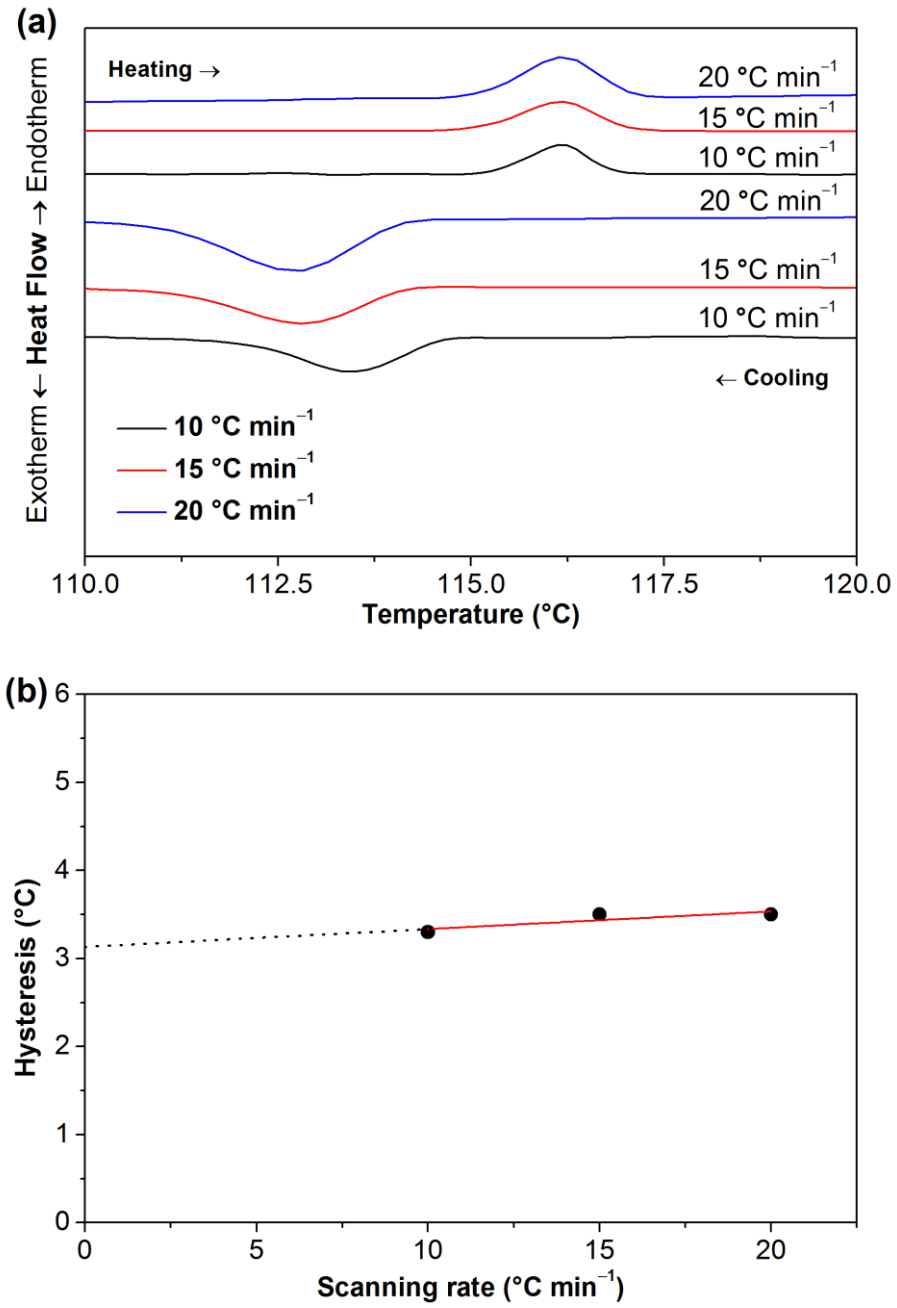

Fig. S7 (a) DSC curves of [Gdm-H][NfO] at different heating/cooling rates showing in particular the phase transition of III → II during the heating scan and the reverse phase transition during the cooling scan; (b) The corresponding limiting temperature hysteresis (3.13 ℃) estimated from the scans extrapolated to a scanning rate of 0 ℃ min^{-1}, demonstrating a first-order solid-solid phase transition.

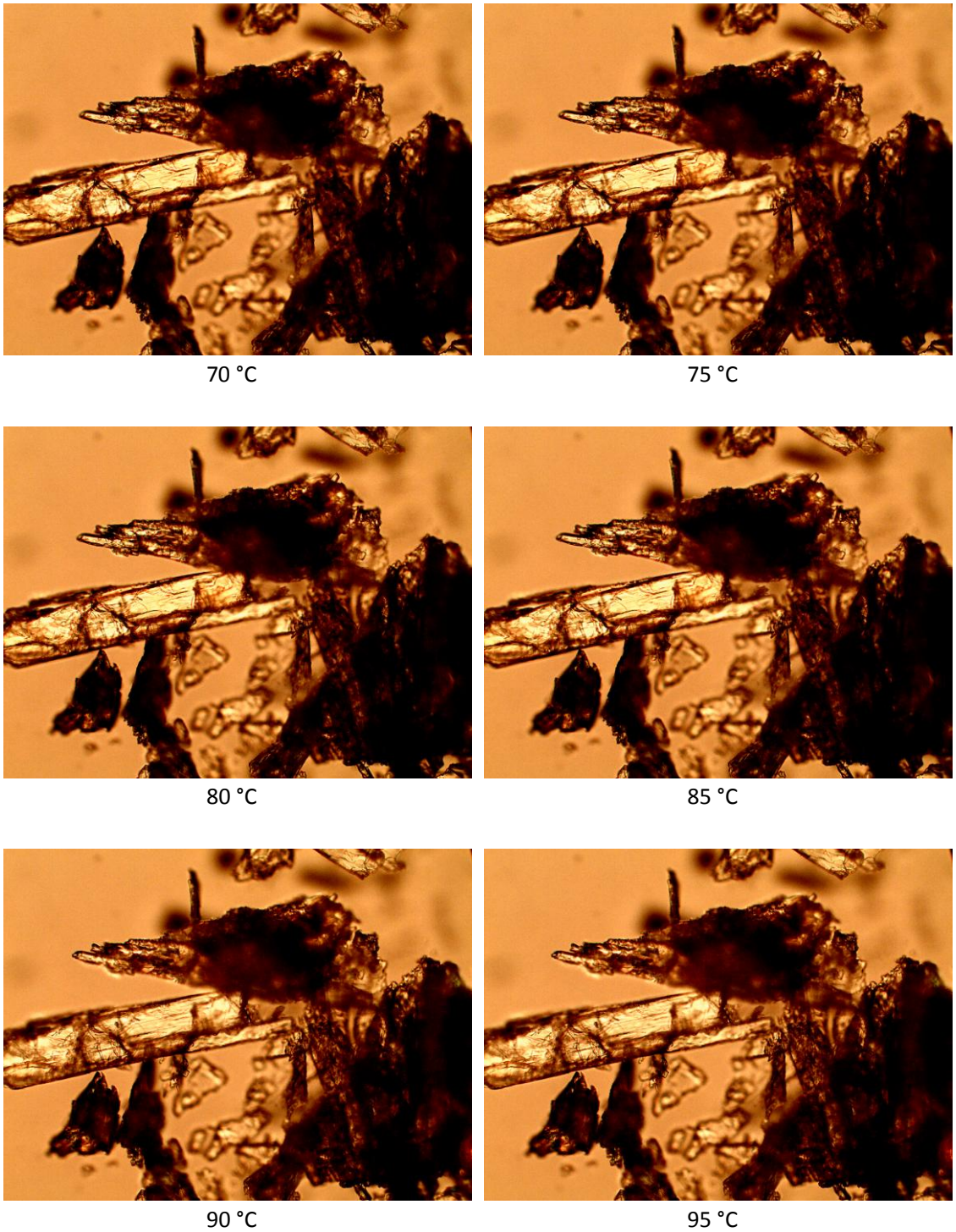

Fig. S8 Morphological changes of tiny crystals of [Gdm-H][NfO] from 80 ℃ to 95 ℃ during the heating scan (5 ℃ min^{-1}) observed via polarized optical microscopy, excluding the possibility of partial melting during the phase transitions of V → IV and IV → III. From 85 ℃ to 90 ℃ the grain boundaries of the rod-like crystal becomes less resolved, corresponding to the phase transition of IV → III with onset temperature of 87.8 ℃ as shown in DSC thermograms (Fig. 7).

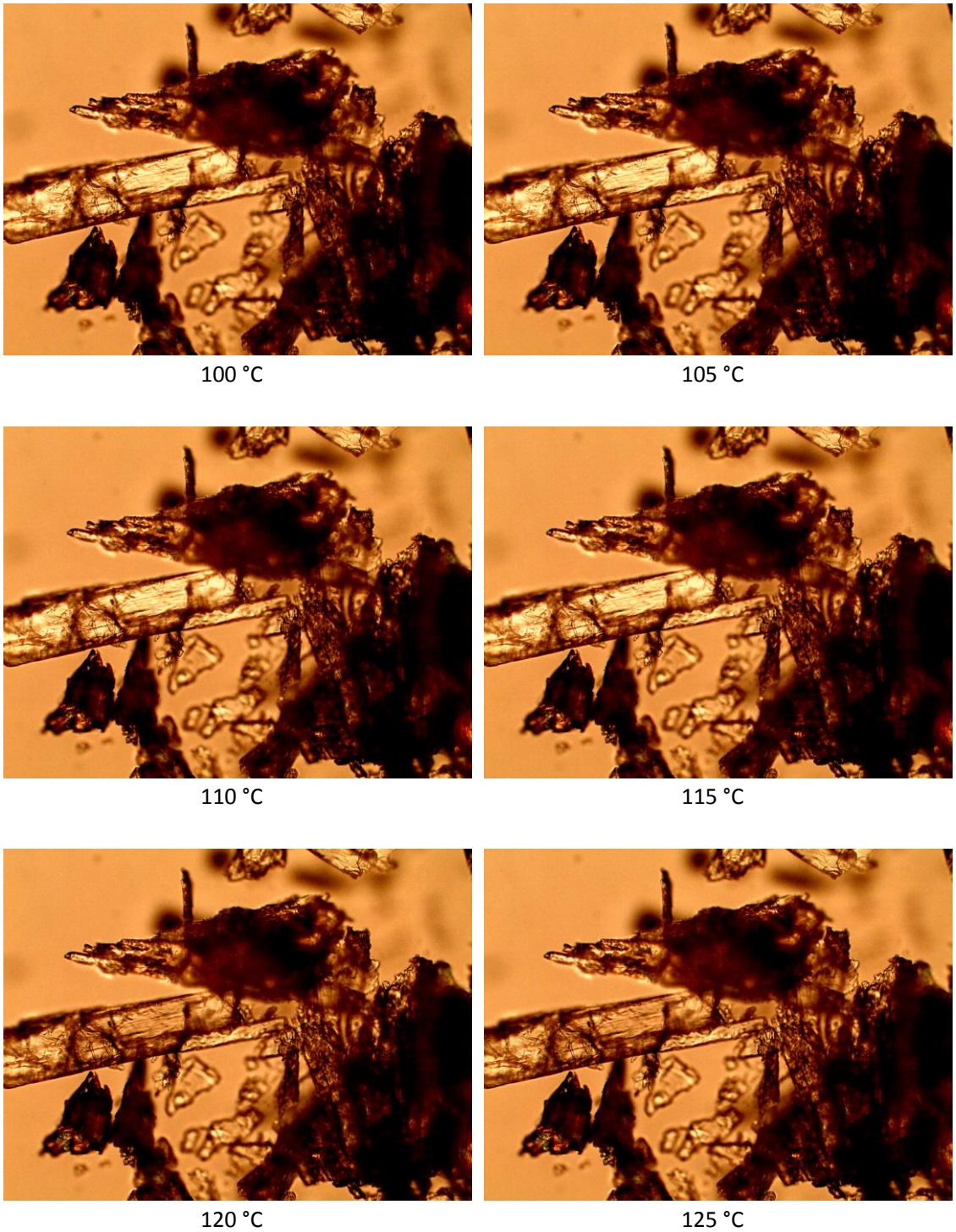

Fig. S9 Morphological changes of tiny crystals of [Gdm-H][NfO] from 100 ℃ to 125 ℃ during the heating scan (5 ℃ min^{-1}) observed via polarized optical microscopy, excluding the possibility of partial melting during the phase transition of III → II. From 115 ℃ to 120 ℃ the color of the rod-like crystal becomes darker, corresponding to the phase transition of III → II with onset temperature of 117.6 ℃ as shown in DSC thermograms (Fig. 7).

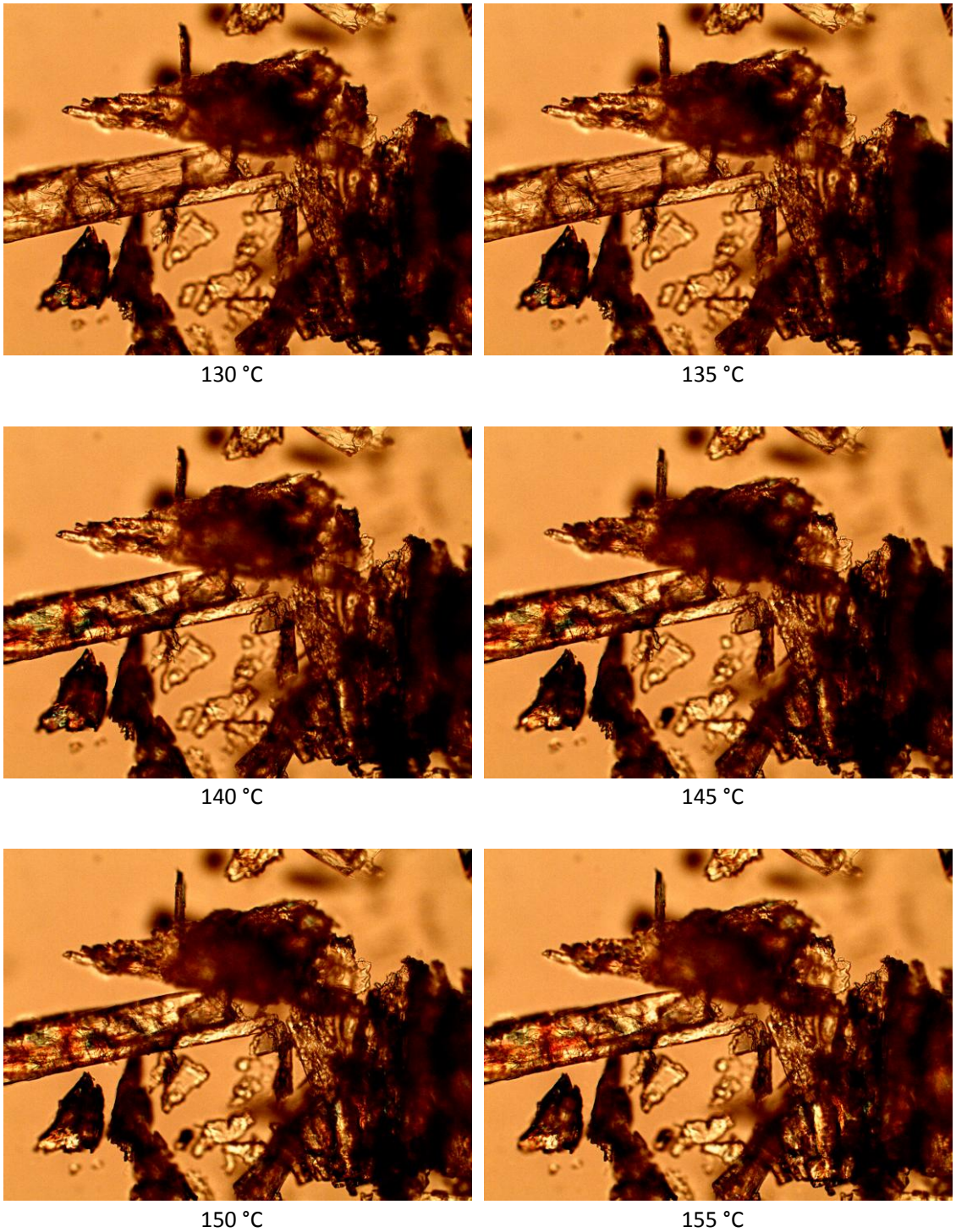

Fig. S10 Morphological changes of tiny crystals of [Gdm-H][NfO] from 130 ℃ to 155 ℃ during the heating scan (5 ℃ min^{-1}) observed via polarized optical microscopy, excluding the possibility of partial melting during the phase transition of II → I. From 135 ℃ to 140 ℃ polarized light begins to appear on the rod-like crystal, corresponding to the phase transition of II → I with onset temperature of 141.9 ℃ as shown in DSC thermograms (Fig. 7).

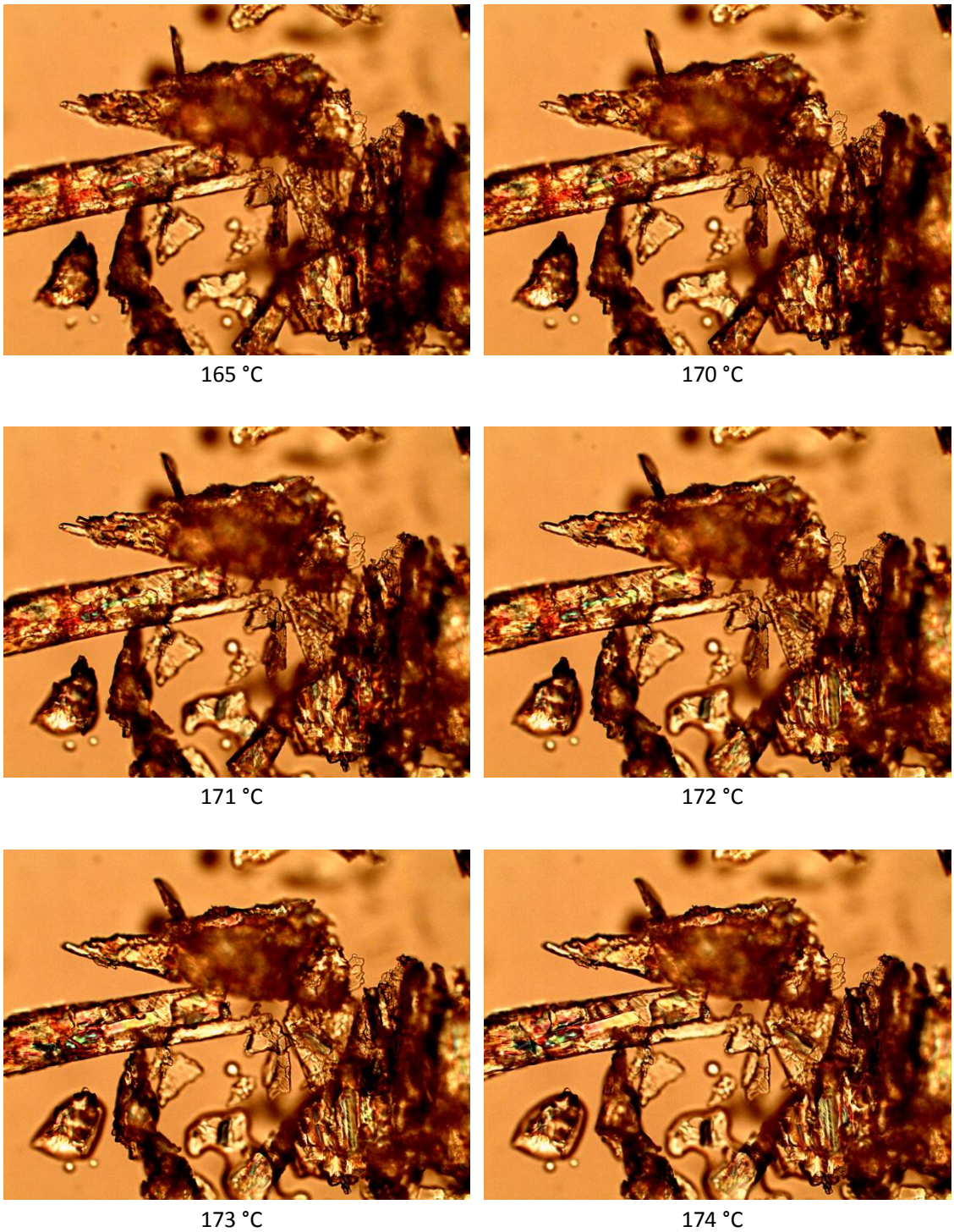

Fig. S11 Morphological changes of tiny crystals of [Gdm-H][NfO] from 165 ℃ to 174 ℃ during the heating scan (5 ℃ min^{-1}) observed via polarized optical microscopy. As from 173 ℃, some crystals (*e.g.* the one on the lower left corner) begin to melt, which corresponds well to the relatively broad and less symmetrical melting peak rather than a sharp transition observed in DSC thermograms (Fig. 7).

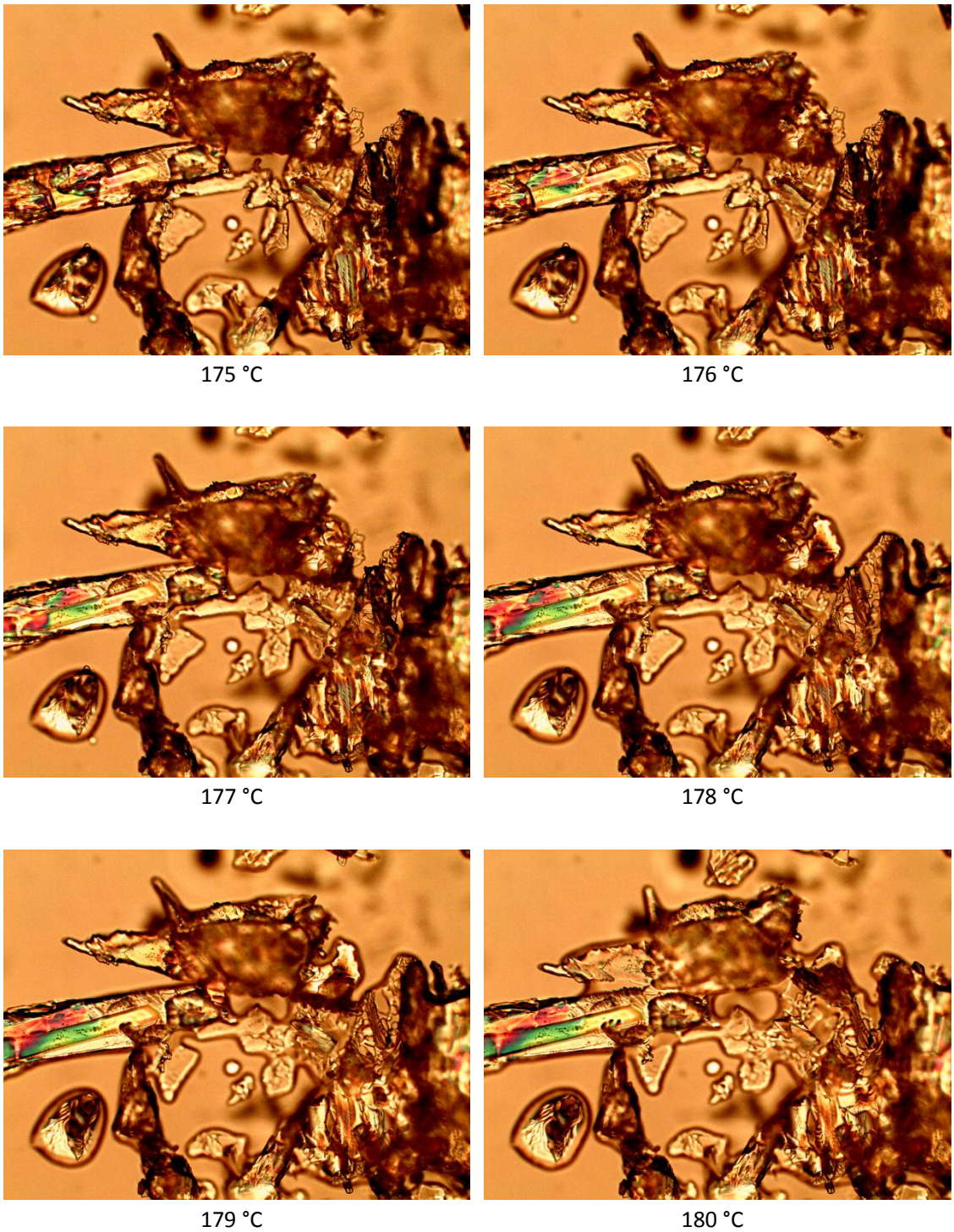

Fig. S12 Morphological changes of tiny crystals of [Gdm-H][NfO] from 175 ℃ to 180 ℃ during the heating scan (5 ℃ min^{-1}) observed via polarized optical microscopy. During this heating period, more crystals begin to melt, corresponding well to the relatively broad and less symmetrical melting peak rather than a sharp transition observed in DSC thermograms (Fig. 7). In particular, some single crystals (*e.g.* the one on the lower left corner) are observed to swim in a melt, indicating clearly partial melting. Note that the oneset temperature and peak temperature of melting in DSC thermograms (Fig. 7) are 186.2 ℃ and 190 ℃, respectively.

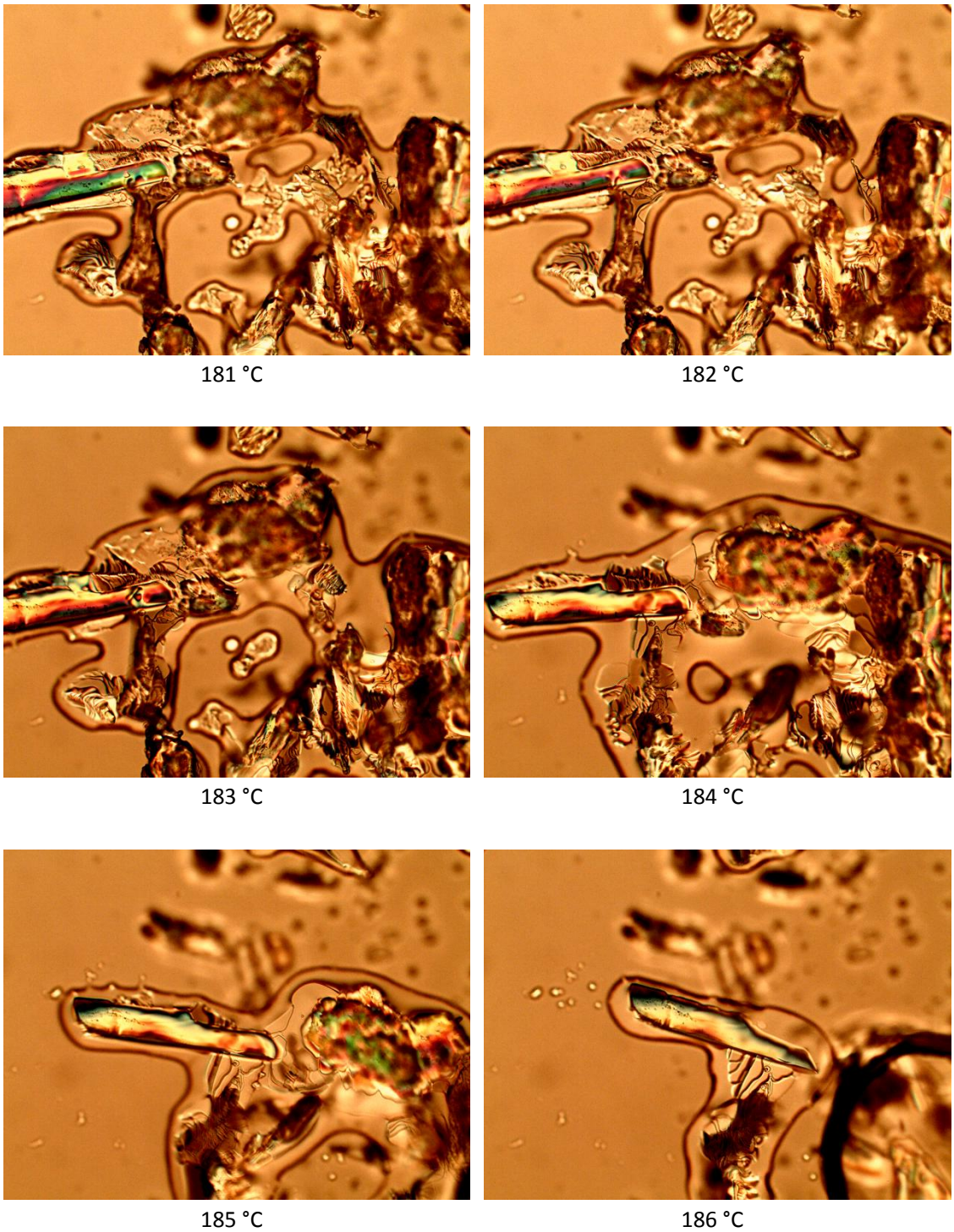

Fig. S13 Morphological changes of tiny crystals of [Gdm-H][NfO] from 181 ℃ to 186 ℃ during the heating scan (5 ℃ min^{-1}) observed via polarized optical microscopy. Clearly, prior to the oneset temperature of melting at 186.2 ℃ in DSC thermograms (Fig. 7), the sample has become a mixture of crystals and melts with some single crystals swimming in the melts.

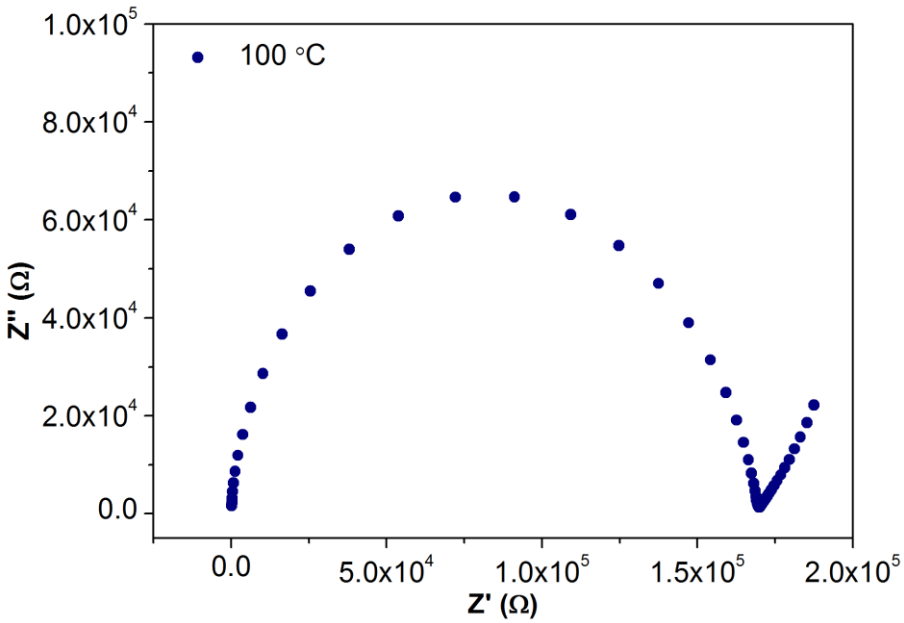

Fig. S14 Nyquist plot for the impedance data derived from the dielectric spectrum at 100 ℃.

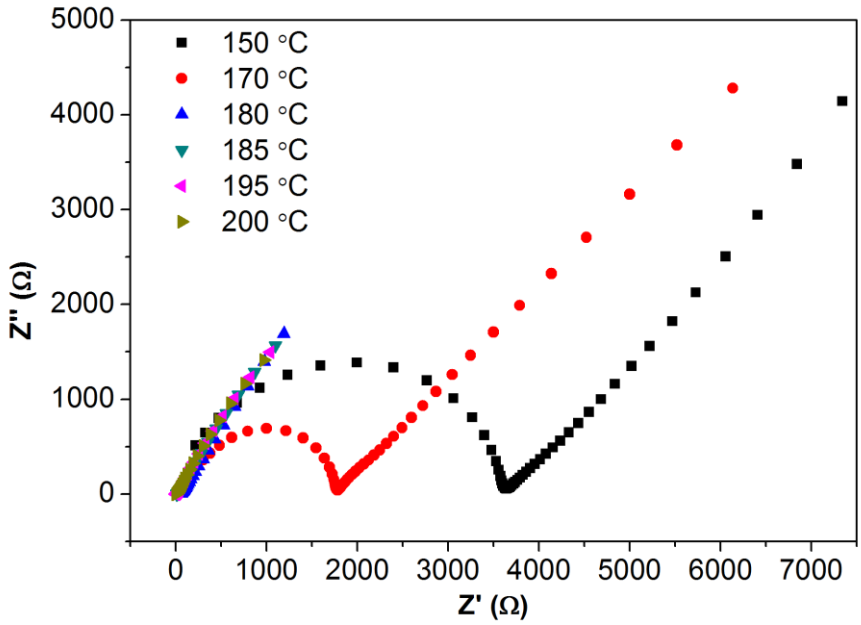

Fig. S15 Nyquist plots for the impedance data derived from the dielectric spectra at 150, 170, 180, 185, 195 and 200 ℃.

References:

[1] http://sdbs.db.aist.go.jp/sdbs/cgi-bin/direct_frame_top.cgi.